HTML ABSTRACT • LINKS

Self-assembled infrared-luminescent Er–Si–O crystallites on silicon

H. Isshiki
FOM Institute for Atomic and Molecular Physics, Kruislaan 407, 1098 SJ Amsterdam, The Netherlands, and The University of Electro-communications, Tokyo 182 8585, Japan

M. J. A. de Dood and A. Polman[a)]
FOM Institute for Atomic and Molecular Physics, Kruislaan 407, 1098 SJ Amsterdam, The Netherlands

T. Kimura
The University of Electro-communications, Tokyo 182 8585, Japan

(Received 6 October 2003; accepted 10 August 2004)

Optically active and electrically excitable erbium complexes on silicon are made by wet-chemical synthesis. The single-crystalline Er–Si–O compound is formed by coating a Si(100) substrate with an $ErCl_3$/ethanol solution, followed by rapid thermal oxidation and annealing. Room-temperature Er-related 1.53 μm photoluminescence is observed with a peak linewidth as small as 4 meV. The complexes can be excited directly into the Er intra-4f states, or indirectly, through photocarriers. Er concentrations as high as 14 at. % are achieved, incorporated in a crystalline lattice with a 0.9 nm periodicity. Thermal quenching at room temperature is only a factor 5, and the lifetime at 1.535 μm is 200 μs. © *2004 American Institute of Physics*. [DOI: 10.1063/1.1814814]

Silicon is a very inefficient light emitter, due to its indirect band gap. However, by adding optically active impurities such as erbium, Si can be made luminescent. In Er-doped silicon, optically or electrically generated electrical carriers can recombine at Er-related carrier traps and then excite the luminescent intra-4f states of Er^{3+} by an impurity Auger process. In an ideal case (low Er concentration, low pump power, and temperature) photoluminescence quantum efficiencies of Si:Er as high as 10% can be achieved.[1] Practical structures, however, such as Er-doped Si light-emitting $p-n$ diodes, suffer from low quantum efficiency (10^{-3}) and low output power,[2] too low for most practical applications. This is the result of the low solubility of Er in Si, as well as phonon-assisted energy backtransfer and Auger quenching that reduce the Er emission efficiency at room temperature. These effects, combined with the small peak emission cross section of Si:Er at room temperature, make Si:Er unsuited for the fabrication of a silicon-based laser or optical amplifier.

To fabricate such devices based on silicon a radically new approach is required. Ideally, Er should be incorporated in a host that can sustain high Er concentrations, while the direct surrounding of the Er should not render it a dopant, so that no Auger quenching occurs. These two requirements point to an insulating host material. In addition, the large band gap typical for an insulator will result in very small thermal quenching. At the same time, the host material should be in intimate contact with silicon, so that electrical excitation is possible. Different types of Si nanostructures integrated with Er-doped SiO_2 have been studied recently that fulfill part of these requirements. For example, Si nanocrystals embedded in Er-doped SiO_2 can act as a sensitizer for Er.[3] However, these isolated nanocrystals cannot be efficiently addressed electrically. This problem may be solved by using Si-rich SiO_2 as the matrix, or by using Er-doped porous Si nanostructures, through which electrical current injection is possible to some degree.[4] Also, multilayer structures have been made, in which Er-doped SiO_2 films are sandwiched between thin Si films from which excitonic coupling to the Er could be achieved.[5] However, none of these structures solve the concentration problem: the concentration of optically active Er in SiO_2 is typically limited to $\sim$1 at. % due to concentration quenching[6] and precipitation.[7] This is too low to produce sufficient gain to overcome waveguide losses in most Si-based materials, and thus so far with these materials an Er-doped Si-based waveguide laser or amplifier has not been made.

In this letter, we present a material that may solve many of the problems encountered with erbium doping of crystalline silicon. It is a single-crystalline structure composed of erbium, oxygen, and silicon, that is fabricated as ultrathin precipitates on the surface of a Si wafer. Er concentrations as high as 14 at. % are achieved. Room temperature photoluminescence (PL) is observed with extremely narrow linewidth. The Er–Si–O crystals on Si can be electrically addressed, and relatively small temperature quenching is observed.

A single-crystal Czochralski-grown n-type silicon wafer ((100) oriented, P-doped, 5 Ω cm) was used as a starting material. The Si wafer was dipped in a 5% HF solution rendering the surface hydrophobic. A uniform layer of $ErCl_3$ was spin-coated on the substrate using an $ErCl_3$/ethanol solution (3000 rpm for 1 min). The $ErCl_3$ solution was obtained by a tenfold dilution of a saturated $ErCl_3$/ethanol solution with ethanol. Subsequently, a two-step annealing process was carried out in a rapid thermal annealing furnace at a heating rate $>$100 °C/s. First, rapid thermal oxidation was performed for 4 min in O_2 flow at 900 °C at a pressure of 1 atm. Subsequently, after a short interval to change the gas flow, rapid thermal annealing at 1200 °C for 3 min was carried out in Ar flow at 1 atm. This sample is denoted RTOA. Reference samples that only received the oxidation anneal (RTO) were also made.

Figure 1 shows Rutherford backscattering spectrometry (RBS) spectra of RTO and RTOA samples taken in [100] channeling configuration. A 2 MeV He beam with a

[a)]Electronic mail: polman@ amolf.nl

 © 2004 American Institute of Physics
Downloaded 09 Nov 2004 to 192.87.153.197. Redistribution subject to AIP license or copyright, see http://apl.aip.org/apl/copyright.jsp

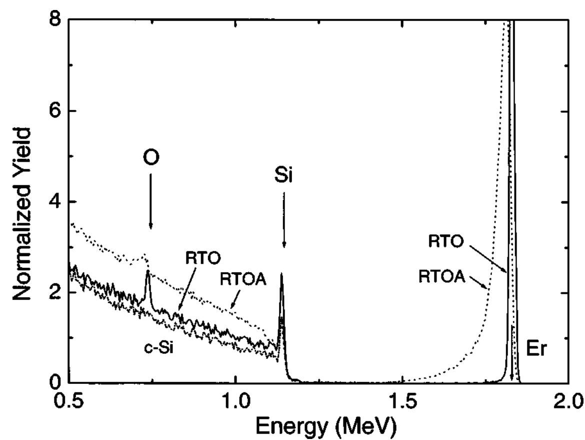

FIG. 1. RBS channeling spectra (2 MeV He, scattering angle 165°) of RTO, RTOA, and *c*-Si(100) samples. The arrows indicate the surface channels for Er, Si, and O.

2-mm-diam spot size on the sample was used. He ions backscattered at an angle of 165° were analyzed using a surface barrier detector with an energy resolution of 14 keV. A channeling spectrum of a Si(100) single crystal reference (*c*-Si) is also shown for comparison. When compared to the single-crystal reference, the spectra for RTO and RTOA samples both show enhanced Er, Si, and O yields.

For the RTO sample, narrow Er, Si, and O surface peaks are observed, all with a width limited by the detector resolution, and channeling is observed in the Si substrate. These data indicate that the RTO process forms an Er–Si–O compound layer at the surface. Assuming, as a first estimate, an $Er_2O_3-SiO_2$ composition, the effective layer thickness estimated from the peak yields is ~4 nm.

For the RTOA sample (oxidation+postanneal), erbium and oxygen profiles in Fig. 1 appear spread out in depth. Figure 2(a) shows a bright-field cross-section transmission electron microscopy (TEM) micrograph of this sample, taken using a 300 keV electron microscope. The image reveals discrete islands on the sample surface, with lateral widths ranging between 30 and 400 nm, and a height between 20 and 120 nm. The surface coverage is about 15%. Energy-dispersive x-ray (EDX) analysis revealed that the islands contain erbium, silicon, and oxygen, no Er signal was observed from the substrate. These data indicate that the Er and O distributions observed in RBS for the RTOA sample are the result of the varying thickness of a multitude of islands across the RBS beam spot. The RBS profiles for Er, Si, and O correspond to a depth extension to 160 nm, in agreement with the thicknesses derived from the TEM data.

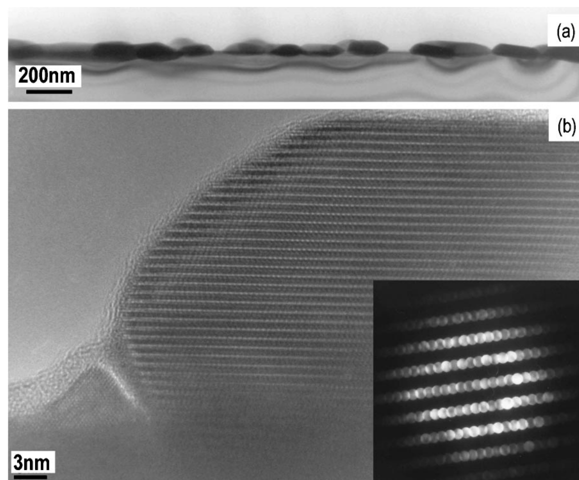

FIG. 2. (a) Bright-field cross-sectional TEM micrograph of the RTOA sample. (b) High-resolution cross-section TEM image of the RTOA sample. Inset: selected area diffraction pattern.

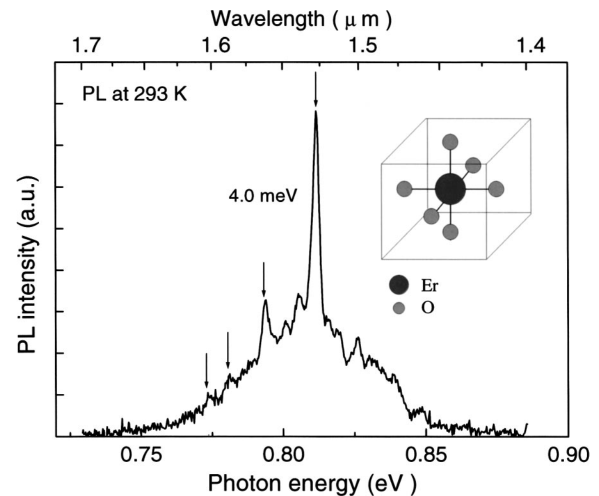

FIG. 3. Room-temperature photoluminescence spectrum of Er–Si–O crystals on Si under 488 nm excitation (pump power 100 mW). The inset shows a schematic of an $Er-O_6$ octahedron.

It is well known that $ErCl_3$ decomposes below 800 °C and given the strong reactivity of Er with O it can be assumed that during the first RTO anneal a surface Er–O compound layer forms (melting point of Er_2O_3 is 2300 °C). From RBS and EDX it follows that this layer is Si-rich. The occurrence of a reaction between Er and O is supported by the fact that similar depth profiles are observed in RBS for Er and O. Then, upon annealing at 1200 °C in the second RTA step, this layer may break up to form the Er–Si–O islands. Indeed, the diffusion coefficient of Er in Si is large enough (and will be further enhanced at the surface) to account for such long-distance material agglomeration. Considering the average surface composition determined by RBS and the island coverage from TEM, the island composition can be roughly estimated to be Er:Si:O=1:2:4, with an Er peak concentration of 14 at. % Figure 2(b) shows a high-resolution cross-sectional image of one of the Er–Si–O precipitates. A selected-area diffraction pattern shown in the inset reveals that the precipitate has a monoclinic single-crystalline structure. The diffraction spots indicate *d* spacings of 0.868 and 0.304 nm and an angle of 83°. These values could not be identified to one of the known erbium silicates. The layered structure shown in Fig. 2(b) is reminiscent of the layered structure with $Er-O_6$ octahedra typical for erbium disilicates.[8] The bending contours observed in the Si substrate beneath the islands in Fig. 2(a) are most likely caused by stress in the substrate, possibly induced by coherent growth of the precipitates on the Si(100) substrate.

Figure 3 shows the room-temperature PL spectrum of the RTOA sample taken using excitation by the 488 nm line of an Ar ion laser at a power of 100 mW. A sharp main peak is observed at 1.529 μm, with a full width at half-maximum of 7.5 nm (4.0 meV). This linewidth is much narrower than that observed for other Er-doped Si-based materials at room temperature, which is typically ~50 nm (26 meV). The PL fine structure is characteristic for transitions between the Stark-

Downloaded 09 Nov 2004 to 192.87.153.197. Redistribution subject to AIP license or copyright, see http://apl.aip.org/apl/copyright.jsp

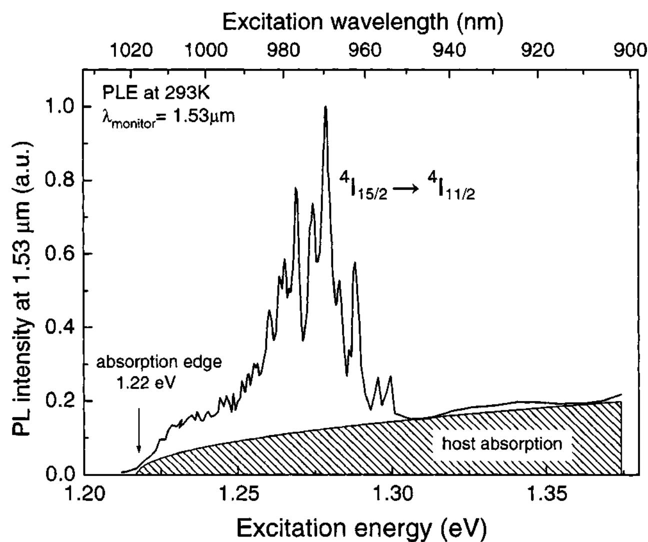

FIG. 4. Room-temperature photoluminescence excitation spectrum of Er–Si–O crystals on Si. The 1.53 μm photoluminescence is monitored as a function of pump wavelength.

split $^4I_{13/2}$ and $^4I_{15/2}$ manifolds of Er^{3+} in a crystalline environment. The splitting behavior is similar to that of Y_2SiO_5:Er[9] and Er_2O_3 (Ref. 10) crystalline compounds in which Er is sixfold coordinated with oxygen atoms (see the inset in Fig. 3). Details of the Stark splitting spectroscopy are described in Ref. 11.

Figure 4 shows a PL excitation spectrum of the RTOA sample, taken by monitoring the peak intensity at 1.53 μm while scanning a Ti:sapphire pump laser in the wavelength range 900–1025 nm, using a power in the range 50–100 mW. The PL intensities were normalized to pump power. A sharply peaked structure is observed, assigned to direct absorption into the Er $^4I_{11/2}$ manifold, and again reflects the crystalline nature of the host. The excitation spectrum also shows a clear Er emission component outside the Er absorption band ($E > 1.30$ eV in Fig. 4). This indicates that Er ions can also be excited through a photocarrier-mediated process. The cross-hatched region in Fig. 4 is a parabolic fit to represent the density of states in the matrix that indicates this indirect component. The apparent absorption edge is near 1.22 eV, well above the bulk Si band gap at room temperature (1.12 eV).

Temperature-dependent PL intensity and lifetime measurements were also performed, using an excitation source at 476.5 nm. The PL intensity decreases by a factor 5 by increasing the temperature from 20 to 290 K, while the lifetime remains constant at 200 μs over this temperature range. This amount of quenching is small compared to that of Er-doped crystalline Si where factor 30 was observed,[12] and indicates that the coupling between Er and the matrix is relatively weak, i.e., strong enough to excite the Er by photocarriers, but weak enough for the backtransfer rate to be smaller than the radiative decay rate.[13,14]

The lifetime of 200 μs is much longer than that of Er-doped crystalline Si at room temperature.[12] It is comparable to that of Er-doped silica glasses doped at a similar concentration.[15] It is difficult to estimate the internal quantum efficiency, as the radiative rate for this new material is unknown. Given the composition, between Si and SiO_2, the radiative rate is likely between 1 and 10 ms, but asymmetry around the Er site in these crystalline materials may further decrease the radiative lifetime. We thus estimate the internal (intra-4*f*) quantum efficiency to be of order 10%.

More research is required to determine the atomic-scale structure of the Er–Si–O crystals synthesized in this work. We speculate that a self-assembly process leads to the formation of $Er-O_6$ octahedra that order in a layered structure. Indeed, self-assembled layers of $Er-O_6$ octahedra made by using the Verneuil method and oxide sintering of Er_2O_3 and SiO_2 have been observed before.[8] In such a Er–Si–O superlattice, the $Er-O_6$ octahedra may then be separated by Si-rich layers that act as sensitizers for the Er. Quantum confinement in these thin Si-rich layers would then lead to the blueshift as observed in the excitation spectrum of Fig. 4.

Finally, we note that our most recent work has shown that continuous layers of the crystalline Er–Si–O material can be formed on Si(100) using metallo-organic molecular beam epitaxy.[16] We have also shown that porous Si can be infiltrated with the Er–Si–O complexes using the wet chemical synthesis introduced here. Assuming a major fraction of the Er is optically active, these geometries, combined with the high Er content, relatively small thermal quenching, and narrow emission linewidth makes us conclude that the Er–Si–O crystal structure presented in this letter is ideally suited as an active medium in a Si-based Er laser.

This work is part of the research program of FOM, which is financially supported by NWO. It was supported in part by a Grant-in-Aid for Scientific Research from the Ministry of Education, Science, Sports, and Culture of Japan. The authors gratefully acknowledge F. D. Tichelaar and T. R. de Kruijff at the Delft University of Technology for TEM analyses.

[1]F. Priolo, G. Franzò, S. Coffa, and A. Carnera, Phys. Rev. B **57**, 4443 (1998).
[2]S. Coffa, G. Franzò, F. Priolo, A. Pacelli, and A. Lacaita, Appl. Phys. Lett. **73**, 93 (1998).
[3]M. Fujii, M. Yoshida, Y. Kanzawa, S. Hayashi, and K. Yamamoto, Appl. Phys. Lett. **71**, 1198 (1997).
[4]T. Kimura, Y. Nishida, A. Yokoi, and R. Saito, J. Appl. Phys. **83**, 1005 (1998).
[5]J.H. Shin, J.-H. Jhe, S.-Y. Seo, Y. H. Ha, and D.W. Moon, Appl. Phys. Lett. **68**, 3567 (2000).
[6]E. Snoeks, P.G. Kik, and A. Polman, Opt. Mater. (Amsterdam, Neth.) **5**, 159 (1996).
[7]A. Polman, D.C. Jacobson, D.J. Eaglesham, R.C. Kistler, and J.M. Poate, J. Appl. Phys. **70**, 3778 (1991).
[8]Y. Smolin and Y. Shepelev, Acta Crystallogr., Sect. B: Struct. Crystallogr. Cryst. Chem. **26**, 484 (1970).
[9]C. Li, C. Wyon, and R. Moncorge, IEEE J. Quantum Electron. **28**, 1209 (1992).
[10]J.B. Gruber, J.R. Henderson, M. Muramoto, K. Rajnak, and J.G. Conway, J. Chem. Phys. **45**, 477 (1966).
[11]H. Isshiki, A. Polman, and T. Kimura, J. Lumin. **819**, 102 (2003).
[12]S. Coffa, G. Franzò, F. Priolo, A. Polman, and R. Serna, Phys. Rev. B **49**, 16313 (1994).
[13]N. Hamelin, P.G. Kik, J.F. Suyver, K. Kikoin, A. Polman, A. Schonecker, and F.W. Saris, J. Appl. Phys. **88**, 5381 (2000).
[14]T. Kimura, H. Isshiki, S. Ide, T. Shimizu, and T. Ishida, J. Appl. Phys. **93**, 2595 (2003).
[15]E. Snoeks, P.G. Kik, and A. Polman, Opt. Mater. (Amsterdam, Neth.) **5**, 159 (1996).
[16]H. Isshiki and T. Kimura (unpublished).

Downloaded 09 Nov 2004 to 192.87.153.197. Redistribution subject to AIP license or copyright, see http://apl.aip.org/apl/copyright.jsp